Analyzing the Optical Properties of a Conjugated Polymer by the Multimode Brownian Oscillator Model

ARTICLE *in* THE JOURNAL OF PHYSICAL CHEMISTRY A · NOVEMBER 2009

Impact Factor: 2.69 · DOI: 10.1021/jp9073043 · Source: PubMed

3 AUTHORS:

Jun Ye
Institute Of High Performance Computing
28 PUBLICATIONS **377** CITATIONS
SEE PROFILE

Andrew C Grimsdale
Nanyang Technological University
155 PUBLICATIONS **8,190** CITATIONS
SEE PROFILE

Yang Zhao
China Institute of Water Resources and Hy…
150 PUBLICATIONS **1,636** CITATIONS
SEE PROFILE

Analyzing the Optical Properties of a Conjugated Polymer by the Multimode Brownian Oscillator Model

Jun Ye, Andrew C. Grimsdale, and Yang Zhao*

School of Materials Science and Engineering, Nanyang Technological University, Singapore 639798

Received: July 30, 2009; Revised Manuscript Received: November 2, 2009

A multimode Brownian oscillator model has been successfully applied for the first time to model the absorption and emission spectra of a conjugated polymer. Extremely good matches were obtained between the calculated and observed spectra for alkyl- and aryl-substituted indenofluorene-based polymers, revealing the underlying photophysics of the investigated polyindenofluorenes in solution as well as solid thin film. Structure variations, defects, and aggregation effects in polymer are shown to have major impacts on the changes of spectral features according to the MBO analysis. These results confirm that the MBO model is a valid method for analyzing the optical behavior of conjugated systems.

Introduction

Conjugated polymers are of great scientific and industrial interest as the active materials for organic optoelectronic devices such as light-emitting diodes (LEDs),[1] organic photovoltaic devices,[2] and polymer lasers.[3] The ability to model their absorption and emission spectra and how they are affected by molecular vibrations could be of considerable importance in designing and optimizing materials for use in these devices. In particular, such modeling might play a key role in attaining electrically pumped lasing from organic materials, which remains a major unrealized goal of research into conjugated materials. One class of polymers that are of particular interest as emitting materials are those based on bridged phenylenes, as their large band gaps make them blue-emitters.[4] By control of the type and proportion of bridges between the phenylene units, the optical and electrical properties of the polymers can be tuned to optimize their performance in organic electronic devices.[4]

One technique available for modeling the interactions between electronic and vibrational transitions is the multimode Brownian oscillator (MBO) model.[5−8] The MBO model describes the electronic relaxation of a two-level system attached to one (few) primary oscillator(s) which is (are) in turn linearly coupled with a bath of secondary phonons. The coupling of the nuclear coordinates with the optical excitations and electronic relaxation channels in solids can be studied by this model. In the MBO model, an electronic two level system interacts linearly with a few primary nuclear coordinates that are in turn coupled linearly to a bath of secondary harmonic oscillators with a given spectral density. The key parameters of the MBO model are the frequencies of the primary oscillators, the Huang−Rhys factors, and the damping coefficients; other controlling parameters include the temperature and the 0−0 transition energy. The frequency of a primary oscillator controls the energy separation between the zero phonon line (ZPL) and the one-phonon peak while the corresponding Huang−Rhys factor reflects the exciton−phonon coupling strength. The damping coefficient is responsible for the coupling strength of the primary oscillator and the bath modes; therefore it controls the broadening of the ZPL and its phonon side bands (PSBs).

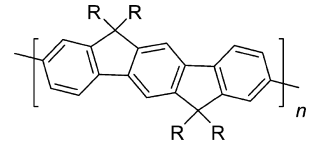

1a R = n-octyl
1b R = 2-ethylhexyl
1c R = 4-octylphenyl

Figure 1. Schematics of PIF derivatives with R representing (**1a**) *n*-octyl-, (**1b**) 2-ethylhexyl-, and (**1c**) 4-octylphenyl functional groups.

This model has been successfully used to interpret spectra of chromophores in liquids and glasses.[5−12] In addition, the model has also been applied to understand the spectra of inorganic systems such as Ce^{3+}-doped yttrium aluminum garnet nanophosphors,[9] InGaN quantum dots,[10] and the ZnO green luminescence band.[11] It has been proven to be a very useful technique for the conceptual understanding of room temperature data on coherence loss due to liquid and solvation dynamics.[12] In the MBO applications, the frequency dependence of the damping coefficient is usually omitted (i.e., Ohmic dissipation) by neglecting the contributions of excited states decay and pure electronic dephasing at low temperatures.[12] Moreover, since the MBO model only considers the coupling of phonons to a two-level system, spectral features that are closely related to the multilevel emission or absorption will not be accurately described by the model.

To our knowledge this model has not been used to interpret the absorption and emission spectra of a conjugated polymer. To test whether the MBO model can be applied to polymers, we chose here to model the spectra of polyindenofluorenes (PIFs, cf. Figure 1),[13] a class of semirigid phenylene-based polymers which have received much less attention than the closely related polyfluorenes (PFs).[14] Like alkyl-substituted PFs, the tetraalkylindenofluorene polymers (**1a** and **1b** in Figure 1) exhibit unstable blue emission in LEDs,[15] which has been shown to be due to formation of an emissive ketone defect.[16] This problem has been overcome by attaching aryl substituents to the bridgeheads as shown in Figure **1c**.[13]

* Corresponding author, yzhao@ntu.edu.sg.

10.1021/jp9073043
Published on Web 11/19/2009

The Brownian Oscillator Model

In the MBO model, the system Hamiltonian can be described by

$$H = |g\rangle H_g \langle g| + |e\rangle H_e \langle e| + H' \quad (1)$$

where

$$H_g = \sum_j \left[\frac{p_j^2}{2m_j} + \frac{1}{2} m_j \omega_j^2 q_j^2 \right] \quad (2)$$

$$H_e = \hbar\omega_{eg}^0 + \sum_j \left[\frac{p_j^2}{2m_j} + \frac{1}{2} m_j \omega_j^2 (q_j + d_j)^2 \right] \quad (3)$$

and

$$H' = \sum_n \left[\frac{P_n^2}{2m_n} + \frac{1}{2} m_n \omega_n^2 \left(Q_n - \sum_j \frac{c_{nj} q_j}{m_n \omega_n^2} \right)^2 \right] \quad (4)$$

In eqs 1−4, P_j (P_n), q_j (Q_n), m_j (m_n), and ω_j (ω_n) are the momentum, coordinate, and mass and angular frequency of the jth (nth) nuclear mode of the primary (bath) oscillators, respectively. In eq 3, d_j is the displacement of the jth nuclear mode in the electronic excited state. The term $\hbar\omega_{eg}^0$ represents the energy difference in the two-level system. H' can be regarded as the coupling between the primary oscillators and bath modes with a coupling strength of c_{nj}. By defining the energy gap operator

$$U = H_e - H_g - \hbar\omega_{eg}^0 \quad (5)$$

the correlation function can be written as

$$C_j(t) = -\frac{1}{2\hbar^2} [\langle U(t)U(0\rho_g)\rangle - \langle U(0)U(t)\rho_g\rangle] \quad (6)$$

In this equation, the operator $U(t)$ is the interaction representation of the operator U and ρ_g is the equilibrium ground-state vibrational density matrix defined as

$$\rho_g = \frac{|g\rangle\langle g| \exp(-\beta \hat{H}_g)}{Tr[\exp(-\beta \hat{H}_g)]} \quad (7)$$

where $\beta = 1/k_B T$. The correlation function in time domain, eq 6, can be converted to frequency domain by the Fourier transform, and its imaginary part in frequency domain is known as the spectral density

$$\tilde{C}_j''(\omega) = \frac{2\lambda_j \omega_j^2 \omega \gamma_j(\omega)}{\omega^2 \gamma_j^2(\omega) + [\omega_j^2 + \omega\Gamma_j(\omega) - \omega^2]^2} \quad (8)$$

where $\Gamma_j(\omega)$ is the real part of the self-energy and the Stokes shift contribution of the jth mode $2\lambda_j$ is described by

$$2\lambda_j = \frac{m_j \omega_j^2 d_j^2}{\hbar} \quad (9)$$

Alternatively, we can write $\lambda_j = S_j \hbar\omega_j$, where S_j is the dimensionless Huang−Rhys factor describing the exciton−phonon interaction strength. We adopt a simple form of the MBO model in this work. In this model, the spectral distribution function $\gamma_j(\omega)$ is assumed to be in its Ohmic limit (i.e., $\gamma_j(\omega) =$ constants). Under these simplifications, the spectral density function for the jth primary oscillator has the following form

$$C_j''(\omega) = \frac{2\lambda_j \omega_j^2 \omega \gamma_j}{\omega^2 \gamma_j^2 + (\omega_j^2 - \omega^2)^2} \quad (10)$$

with the self-energy term $\Gamma_j(\omega)$ set to zero.

The spectral response function $g(t)$ can be expressed in terms of the correlation function described in eq 10 as

$$g(t) = \frac{1}{2\pi} \int_{-\infty}^{\infty} d\omega \frac{C''(\omega)}{\omega^2} [1 + \coth(\beta\hbar\omega/2)](e^{-i\omega t} + i\omega t - 1) \quad (11)$$

The function $C''(\omega)$is a summation of individual contributions from each primary oscillator

$$C''(\omega) = \sum_j C''_j(\omega) \quad (12)$$

The PL line shape then can be calculated from

$$I_{PL}(\omega) = \frac{1}{\pi} \mathrm{Re} \int_0^{\infty} \exp[i(\omega - \omega_{eg} + \lambda)t - g^*(t)]\, dt \quad (13)$$

with

$$\lambda = \sum_j \lambda_j$$

The Fitting Procedure

Initialization of S_2, ω_2, γ_2, and E_{eg}. The relative ratio between the highest peak and the second highest one is determined first from the solution spectra, where the value of the ratio is used as the initial value of S_2 for each material. For the thin-film spectra, the procedure of obtaining an initial value of S_2 is similar, but care must be taken for the spectra with irregular shapes or non-Poisson distributions (e.g., PL spectra for PIF-OCT and PIF-EH thin film). The initial value of ω_2 in our fitting is usually taken as the spacing between the highest and the next highest peaks. The initial value of γ_2 is determined by the overall line shape of the spectra (underdamped or overdamped). For the underdamped spectra as shown in Figure 2, the initial value of γ_2 is usually taken as one-third of ω_2. Finally, the initial value of E_{eg} is determined by the position of ZPL of a spectrum.

Initialization of S_1, ω_1, and γ_1. Low-energy modes strongly coupled to the electronic transition provide additional broadening of the peaks. After the initialization of high-energy modes, the spectra without adding low-energy modes have been compared to experimental ones. The difference will provide a rough guide on how to proceed. The initial values of S_1 and ω_1 are usually taken as 1 (strong coupling) and 100 cm^{-1} (according to ref 17), respectively. Furthermore, since the thermal energy at room temperature (~25 meV) is much higher than the energy of these low energy modes (~12 meV), the overall line shape is not sensitive to γ_1. Thus the absolute value for γ_1 obtained by solely fitting room-temperature spectra may not be very meaningful. In this case, one could take γ_1 closer to γ_2 as an initial value.

Results and Discussion

The synthesis of the polymers[13,15] and the recording of their absorption and emission spectra[16] have been previously described elsewhere. The samples of the alkylated polymers **1a** and **1b** were ones in which great care was taken during synthesis to avoid formation of the ketone defect so that their emission spectra displayed no apparent sign of the defect emission that has previously been observed (especially from polymer **1a**).[15]

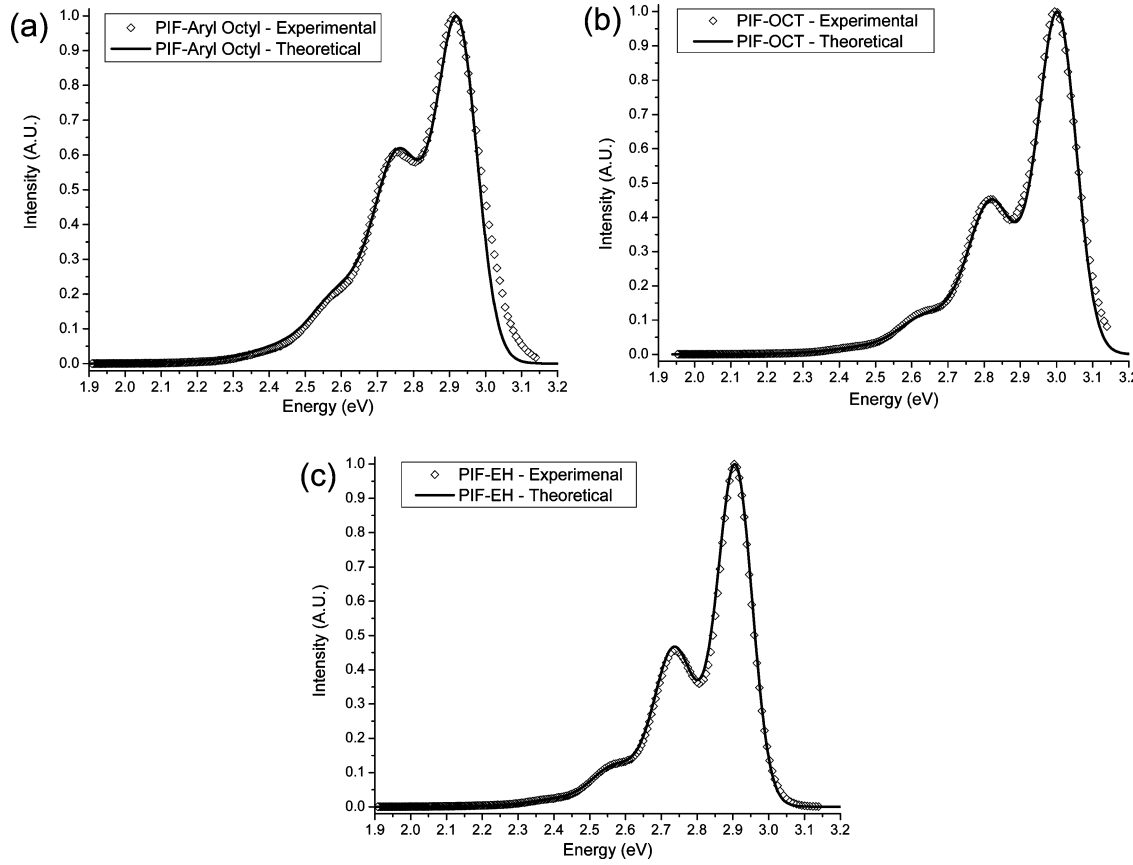

Figure 2. The experimental[16] and MBO PL spectra for (a) PIF−Aryl Octyl, (b) PIF−OCT, and (c) PIF−EH in dilute toluene solution. The parameters for the MBO calculations are taken from Table 1.

TABLE 1: Fitted MBO Parameters for the PL Spectra of the PIFs in Toluene Solution (T = 300 K)

sample	ω_1 (cm^{-1})	ω_2 (cm^{-1})	γ_1 (cm^{-1})	γ_2 (cm^{-1})	S_1	S_2	E_{eg} (eV)
PIF−Aryl Octyl	153	1450	300	360	2.8	0.70	2.980
PIF−OCT	147	1585	310	360	2.7	0.54	3.055
PIF−EH	110	1450	300	280	3.0	0.55	2.950

TABLE 2: Fitted MBO Parameters for the PL Spectra of the PIF Thin Films (T = 300 K)

sample	ω_1 (cm^{-1})	$\omega_{2(3)}$ (cm^{-1})	γ_1 (cm^{-1})	$\gamma_{2(3)}$ (cm^{-1})	S_1	$S_{2(3)}$	E_{eg} (eV)
PIF−Aryl Octyl	120	1440	350	340	2.6	0.855	2.905
PIF−OCT(1)[a]	75	1280 (630)	400	120 (240)	1.5	0.63 (0.27)	2.810
PIF−OCT(2)[b]	75	1200	400	500	1.5	1.00	2.430
PIF−EH(1)	90	1200	350	400	2.8	0.70	2.900
PIF−EH(2)[c]	90	1700	350	360	2.8	0.36	2.775
PIF−EH(3)[c]	90	1500	350	800	2.8	0.80	2.430

[a] A three-mode BO calculation has been performed for the first optical transition with E_{eg} = 2.81 eV. [b] The transition due to the ketone defects in PIF−OCT. [c] Two optical transitions take place in these samples. A weighting factor of 0.05 was applied to the spectra PIF−OCT(2) before being added to PIF−OCT(1) to obtain the final MBO spectrum. For the final MBO spectrum of PIF−EH, weighting factors of 0.38 and 0.09 were applied to PIF−EH(2) and PIF−EH(3), respectively, before being added to PIF−EH(1).

The previously recorded spectra of these materials were replotted with the x-axis showing photon energy in electronvolts (eV) (instead of wavelength in nanometers as previously published[16]) for spectral comparison with the MBO model.

In order to describe the PL spectra of the polymers, we first introduce two phonon modes for the MBO fittings. In this scheme, there is one low-frequency phonon mode with a large S and one high-frequency mode with a small S. The introduction of the relatively strongly coupled low-frequency modes (∼100 cm^{-1}, usually low-energy torsional twisting and chain stretching modes[17]) is necessary in order to adequately account for the broadening of the ZPLs and PSBs observed experimentally, while the overall line shape of a spectrum is determined by the coupling of the high-frequency mode with the electronic transition. The parameters used to perform the MBO calculations are listed in Tables 1 and 2. As can be seen from Figure 2, the MBO spectra match the observed ones extremely well, thus demonstrating the validity of the MBO model for interpreting the optical processes of conjugated polymers in dilute solutions. However, the situation becomes more complicated when the polymers are fabricated in the form of thin films. According to the time-resolved fluorescence spectroscopy in ref 16, new peaks for pristine thin films of the polymers were observed compared to their solution spectra. The new peaks around 2.4 eV were ascribed to ketone defects formed during the synthesis of PIF−OCT and PIF−EH.[4,16] From Figure 2b of ref 16, there is

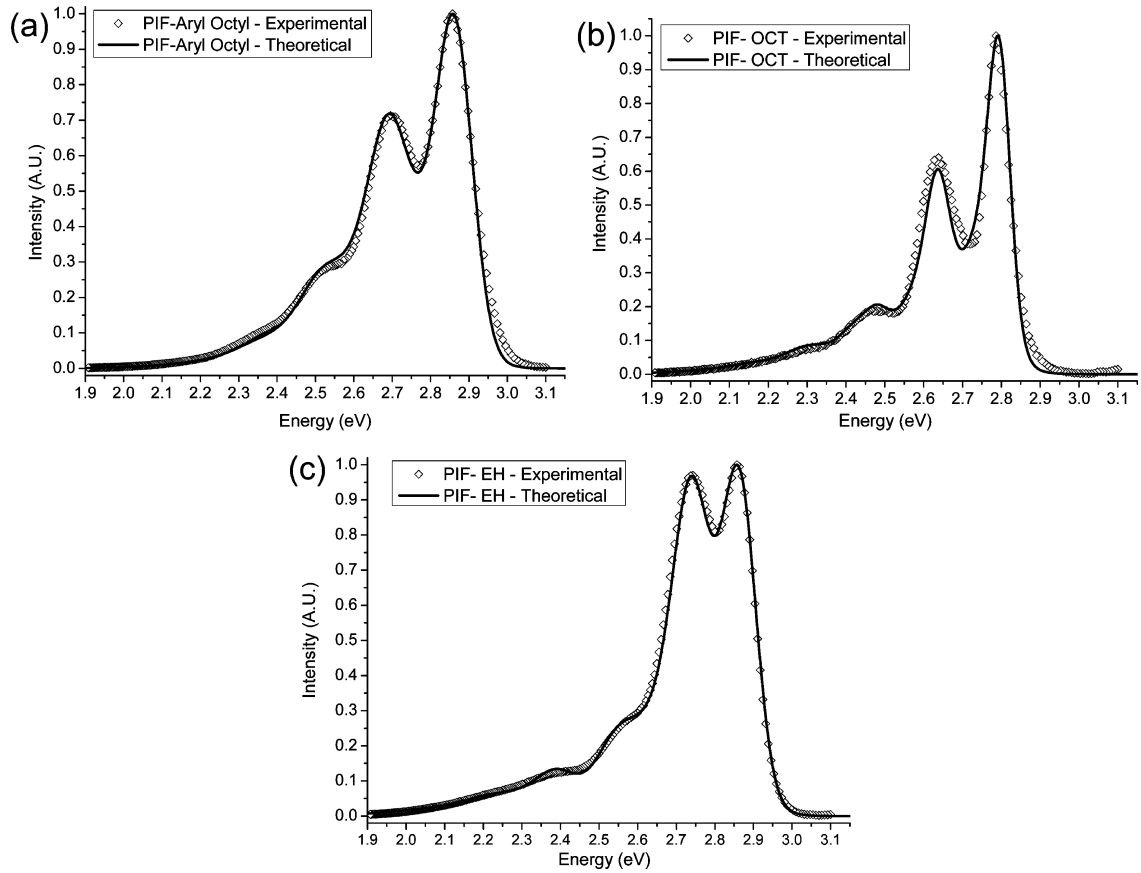

Figure 3. The experimental[16] and MBO PL spectra for (a) PIF−Aryl Octyl, (b) PIF−OCT, and (c) PIF−EH thin films. The parameters for the MBO calculations are taken from Table 2.

also an additional peak located around 2.7 eV for PIF−EH, the origin of which may lie in the formation of aggregation sites due to short-range order of this polymer in the solid state. From the results of ref 16 and the discussions above, we adopt a different approach to fit the PL spectra of PIF−OCT and PIF−EH thin films in order to take into account the effects of defects and aggregation. The fitting parameters in Table 2 were chosen accordingly. Note that the MBO parameters for the PIF−Aryl Octyl thin film spectra are similar to the solution case due to the fact that there should be no ketone defects present in this material.[16] Furthermore, the final spectra of PIF−OCT and PIF−EH thin films are the result of a summation of various contributions with specific weighting factors. The weighting factors of these additional emission features are chosen according to the concentrations of defects and aggregation sites that are responsible for the emission lines. As suggested in ref 16, the lifetime of the PL emission in pristine thin films of PIF−EH is rather short compared to those in PIF−OCT and PIF−Aryl Octyl, and therefore, it is expected that PIF−EH will have a higher concentration of ketone defects. This is reflected by a higher value of weighting factor for PIF−EH(3) (0.09) than that for PIF−OCT(2) (0.05).

The MBO spectra for PIFs in the solid state also match the experimental spectra very well, demonstrating the importance of the emission features due to defects and aggregation in the spectra of PIF−OCT and PIF−EH (cf. Figure 3, parts b and c). Compared to Figure 2, the PL spectra in Figure 3 have been changed significantly, especially for PIF−OCT and PIF−EH. By comparison of the parameters in Tables 1 and 2, it can be found that the spectra of PIF solid thin films share common features of red-shifted singlet PL emissions, slightly increased Huang−Rhys factors, reduced primary phonon frequencies, as well as peak-narrowing.

The red shifts of the PL spectra of thin film PIFs reflect the enhancement of the interchain interactions in the solid state, where the strength of the interactions can be described by absolute value of the shift. The MBO results indicate that the interchain interaction strengths fall in the following order: PIF−OCT (0.245 eV) > PIF−Aryl Octyl (0.075 eV) > PIF−EH (0.050 eV), where the numbers in parentheses are the absolute values of the shifts. These results are in qualitatively agreement with those in ref 16, where the interchain interactions have been minimized in PIF−EH due to the formation of a cylindrical shell surrounding the polymer backbone.

The obtained values of the Huang−Rhys factor S suggest that the exciton−phonon coupling in the PIFs is weak and PIF−Aryl Octyl has a significantly larger coupling strength than the other two samples. The Huang−Rhys factor is also found to increase once the polymers are fabricated in the solid thin film form. This may be mainly due to an increase of localization lengths[18] in the pristine films. Similar trends are also found in other polymer systems such as polyfluorenes,[19] where a decrease of S is proposed for the annealed or crystallized films as compared to their as-coated counterparts. The ordering of S (i.e., PIF−Aryl Octyl > PIF−EH > PIF−OCT) does not change as one goes from solutions to solid films, indicating the role the polymer structure plays in determining the exciton−phonon coupling strength. The largest S is found for PIF−Aryl Octyl both in solutions and in solid thin films, and therefore, a relatively large reorganization energy is expected for this polymer, which may be related to the flexibility of its side chains. The ordering of S also reveals the degree of disorder in

the polymer solid thin films. PIF−OCT, PIF−EH, and PIF−Aryl Octyl were previously found to have long-range order, short-range order, and local amorphous arrangements of macromolecular fragments,[16] respectively. The reduction of S is mainly due to the decreasing of structural deformation of the excited states with the increasing conjugated length.[19] As a result, PIF−OCT in the solid state with the long-rage order is found to have the smallest S value compared to the other two.

Further inspection of Table 2 suggests general softening of the primary phonons, which are closely related to the structural ordering of the polymers in the solid state. Since the PL spectra were measured under room temperature, the degree of thermal disorder is same for the PIFs. The MBO analysis suggests the largest phonon softening ($\sim$305 cm^{-1}) occurs in the PIF−OCT film which possesses long-range order, while the second largest softening ($\sim$250 cm^{-1}) is found in PIF−EH film with short-range order. PIF−Aryl Octyl films with amorphous structure have the least softening ($\sim$10 cm^{-1}). Moreover, the low-frequency phonons also display softening as indicated in Table 2. Such behavior directly leads to the peak narrowing in the thin film spectra compared to the solution cases.

From above discussions, it is clear that the MBO model can be used to interpret photophysics in PIFs in a semiquantitative way, where the parameters obtained can be used as references for more elaborate, quantitative studies. Work is in progress to apply the MBO model to study the spectra of other bridged phenylene polymers, such as polyfluorenes,[14] poly(ladder-type pentaphenylene)s,[20] or ladder-type polyphenylenes.[21]

Conclusions

The MBO model has been used successfully to model the absorption and emission spectra of a conjugated polymer for the first time. The calculated spectra for alkyl and aryl-substituted polyindenofluorenes closely match the observed spectra. The parameters obtained reveal the underlying photophysics of PIFs in solution as well as in solid thin film. The MBO results indicate differences between the PIF spectral line shapes in solutions and solid films are mainly due to their structural differences as well as the presence of ketone defects and aggregation effects. Structural changes introduce variations in the conjugation length and, thus, lead to changes of the Huang−Rhys factor S, while the amount of phonon softening is also found to vary with structural ordering, the presence of ketone defects, and aggregation effects. Despite its conceptual simplicity, the MBO model is still clearly a valid method for understanding the photophysical behavior of conjugated systems. In addition, as one of the authors concluded more than a decade ago in a study of nonlinear optical responses of chromophores weakly coupled to many two-level systems, an often-used model for amorphous materials, the optical response obtained using the second-order cumulant expansion for the spin-bath systems closely resembles that of the MBO model.[6] From this perspective, this MBO model is also expected to be valid if the environment has glassy behavior provided that the bath is not strongly coupled to the chromophores.

References and Notes

(1) (a) Kraft, A.; Grimsdale, A. C.; Holmes, A. B. *Angew. Chem., Int. Ed.* **1998**, *37*, 403. (b) Grimsdale, A. C.; Chan, K. L.; Martin, R. E.; Jokisz, P. G.; Holmes, A. B. *Chem. Rev.* **2009**, *109*, 897.

(2) Günes, S.; Neugebauer, H.; Sariciftci, N. S. *Chem. Rev.* **2007**, *107*, 1324.

(3) Samuel, I. D. W.; Turnbull, G. A. *Chem. Rev.* **2007**, *107*, 1272.

(4) (a) Grimsdale, A. C.; Müllen, K. *Macromol. Rapid Commun.* **2007**, *28*, 1676. (b) Grimsdale, A. C.; Müllen, K. *Adv. Polym. Sci.* **2008**, *212*, 1.

(5) Mukamel, S. *Principles of Nonlinear Optical Spectroscopy*; Oxford University Press: Oxford, 1995.

(6) Zhao, Y.; Chernyak, V.; Mukamel, S. *J. Phys. Chem. A* **1998**, *102*, 6614.

(7) Zhao, Y.; Knox, R. S. *J. Phys. Chem. A* **2000**, *104*, 7751.

(8) Ye, J.; Zhao, Y.; Ng, N.; Cao, J. S. *J. Phys. Chem. B* **2009**, *113*, 5897.

(9) Su, L. T.; et al. *J. Phys. Chem. B* **2008**, *112*, 10830.

(10) Shi, S. L.; et al. *J. Phys. Chem. B* **2006**, *110*, 10475.

(11) Xu, S. J.; et al. *Appl. Phys. Lett.* **2006**, *88*, 083123.

(12) Knox, R. S.; Small, G. J.; Mukamel, S. *Chem. Phys.* **2002**, *281*, 1.

(13) (a) Setayesh, S.; Marsitzky, D.; Müllen, K. *Macromolecules* **2000**, *33*, 2016. (b) Jacob, J.; Zhang, J.; Grimsdale, A. C.; Müllen, K.; Gaal, M. *Macromolecules* **2003**, *36*, 8240.

(14) (a) Neher, D. *Macromol. Rapid Commun.* **2001**, *22*, 1365. (b) Scherf, U.; List, E. J. W. *Adv. Mater.* **2002**, *14*, 477.

(15) Grimsdale, A. C.; Leclere, P.; Lazzaroni, R.; MacKenzie, J. D.; Murphy, C.; Setayesh, S.; Silva, C.; Friend, R. H.; Müllen, K. *Adv. Funct. Mater.* **2002**, *12*, 729.

(16) Keivanidis, P. E.; Jacob, J.; Oldridge, L.; Sonar, P.; Carbonnier, B.; Baluschev, S.; Grimsdale, A. C.; Müllen, K.; Wegner, G. *ChemPhysChem* **2005**, *6*, 1650.

(17) Tretiak, S.; Saxena, A.; Martin, R. L.; Bishop, A. R. *Phys. Rev. Lett.* **2002**, *89*, 097402.

(18) Hagler, T. W.; Pakbaz, K.; Voss, K. F.; Heeger, A. J. *Phys. Rev. B.* **1991**, *44*, 8652.

(19) Asada, K.; Kobayashi, T.; Naito, H. *Thin Solid Films.* **2006**, *499*, 192.

(20) (a) Jacob, J.; Sax, S.; Piok, T.; List, E. J. W.; Grimsdale, A. C.; MüllenK., *J. Am. Chem. Soc.* **2004**, *126*, 6987. (b) Jacob, J.; Grimsdale, A. C.; Müllen, K.; Sax, S.; Gaal, M.; List, E. J. W. *Macromolecules* **2005**, *38*, 9933.

(21) Scherf, U. *J. Mater. Chem.* **1999**, *9*, 1853.

JP9073043